








Article

Omeprazole Promotes Chloride Exclusion and Induces Salt Tolerance in Greenhouse Basil

Petronia Carillo ¹, Pasqualina Woodrow ¹, Giampaolo Raimondi ², Christophe El-Nakhel ², Antonio Pannico ², Marios C. Kyriacou ³, Giuseppe Colla ⁴, Mauro Mori ², Maria Giordano ², Stefania De Pascale ² and Youssef Rouphael ^{2,*}

¹ Department of Environmental, Biological and Pharmaceutical Sciences and Technologies, University of Campania, “Luigi Vanvitelli”, Caserta 81100, Italy

² Department of Agricultural Sciences, University of Naples Federico II, Portici 80055, Italy

³ Department of Vegetable Crops, Agricultural Research Institute, Nicosia 1516, Cyprus

⁴ Department of Agriculture and Forest Sciences, University of Tuscia, Viterbo 01100, Italy

* Correspondence: youssef.rouphael@unina.it; Tel.: +39-(081)-253-9134

Received: 18 May 2019; Accepted: 2 July 2019; Published: 4 July 2019



Abstract: The role of small bioactive molecules (<500 Da) in mechanisms improving resource use efficiency in plants under stress conditions draws increasing interest. One such molecule is omeprazole (OMP), a benzimidazole derivative and inhibitor of animal proton pumps shown to improve nitrate uptake and exclusion of toxic ions, especially of chloride from the cytosol of salt-stressed leaves. Currently, OMP was applied as substrate drench at two rates (0 or 10 μM) on hydroponic basil (*Ocimum basilicum* L. cv. Genovese) grown under decreasing $\text{NO}_3^-:\text{Cl}^-$ ratio (80:20, 60:40, 40:60, or 20:80). Chloride concentration and stomatal resistance increased while transpiration, net CO_2 assimilation rate and beneficial ions (NO_3^- , PO_4^{3-} , and SO_4^{2-}) decreased with reduced $\text{NO}_3^-:\text{Cl}^-$ ratio under the 0 μM OMP treatment. The negative effects of chloride were not only mitigated by the 10 μM OMP application in all treatments, with the exception of 20:80 $\text{NO}_3^-:\text{Cl}^-$, but plant growth at 80:20, 60:40, and 40:60 $\text{NO}_3^-:\text{Cl}^-$ ratios receiving OMP application showed maximum fresh yield (+13%, 24%, and 22%, respectively), shoot (+10%, 25%, and 21%, respectively) and root (+32%, 76%, and 75%, respectively) biomass compared to the corresponding untreated treatments. OMP was not directly involved in ion homeostasis and compartmentalization of vacuolar or apoplasmic chloride. However, it was active in limiting chloride loading into the shoot, as manifested by the lower chloride concentration in the 80:20, 60:40, and 40:60 $\text{NO}_3^-:\text{Cl}^-$ treatments compared to the respective controls (−41%, −37%, and −24%), favoring instead that of nitrate and potassium while also boosting photosynthetic activity. Despite its unequivocally beneficial effect on plants, the large-scale application of OMP is currently limited by the molecule’s high cost. However, further studies are warranted to unravel the molecular mechanisms of OMP-induced reduction of chloride loading to shoot and improved salt tolerance.

Keywords: benzimidazole; chloride toxicity; ion homeostasis; *Ocimum basilicum* L.; photosynthesis; proton pump inhibitor; root-to-shoot; salt tolerance; small bioactive molecules

1. Introduction

Soil salinity affects plants’ growth and yield via pleiotropic mechanisms involving water stress [1–3], ion toxicity and nutrient imbalance [4–7], and oxidative damage [8,9]. When the electrical conductivity (EC) of the soil exceeds the threshold limit of 4 dS m^{-1} , corresponding to about 40 mM of sodium chloride (NaCl), most of the glycophytes, among which vegetable crops, undergo a reduced capacity to absorb water from soil [10,11]. This latter effect translates into a disturbance in plant water relations,

stomatal aperture and transpiration that reduces the expansion of existing leaves and the emergence of new leaves and lateral buds [12]. If the stress persists, excess ions accumulate in the plants causing osmotic and ion specific effects, which interfere with protein synthesis and activity, membrane stability, and electron transport thereby impairing growth and crop productivity [2,12]. One ubiquitous protective mechanism involves the synthesis of small molecules (<500 Da) that are directly or indirectly involved in osmotic balance, and stabilization and protection of membranes and macromolecules by oxidative stress [3,13,14]. Most of these small molecules are nitrogen-containing compounds, such as amino acids, amines, and betaines, or sugars, which, when accumulated in the cytosol, counteract the osmotic and toxic effect of sodium and chloride mostly compartmentalized in the vacuole [15–17].

Moreover, biologically active small molecules, of natural or synthetic origin, can be supplied exogenously at very low concentrations and relieve or protect plants from saline stress [18–21]. Several recent studies have highlighted a beneficial role of omeprazole (OMP), a small molecule of 345 Da, in salinity tolerance [22–25] and mechanical stress tolerance [26]. OMP is a benzimidazole derivative used as a prescribed drug to treat peptic ulcers, gastroesophageal reflux, and other hypersecretory states in humans for its ability in inhibiting the P-type IIC proton pump H^+/K^+ -ATPases in the gastric parietal cell, blocking the final step in the gastric acid secretory pathway [27–29]. Notwithstanding, there is a very low homology between plants and animal proton pumps [22], it has been shown that OMP can act as plant growth regulator improving tolerance to salinity at concentration ranging between 10 and 100 μ M [22,23]. OMP does not directly regulate potassium to sodium ratio and ion homeostasis, but it is able to increase the concentration of nitrate in roots and leaves while reducing those of sodium and chloride in both organs. This increase of nitrate can favor the synthesis and accumulation of N-containing compounds involved in osmotic adjustment and ROS scavenging, improving the physiological functions and viability of salt stressed plants [3]. Moreover, OMP is able to increase root growth and nutrients resource efficiency in control plants [3] and mechanical stressed plants [26]. The involvement of OMP in the regulation of plant radical growth and protection from salt stress certainly entails a complex signaling and/or hormonal action [3,23], determined at the genetic level, as demonstrated by the recent work of Cirillo et al. [25] on two basil contrasting genotypes, that, though, has not yet been unraveled. Cirillo et al. [25] attributed the OMP beneficial effect on the salt sensitive basil genotype Napoletano to this small molecule specific capacity to improve chloride exclusion from the cytosol of salt stressed plants. However, their study, as well as the most of the studies performed on the effects of salinity on plants, have used NaCl as salt, and focused on sodium accumulation and toxicity, considering sodium as the main problem responsible for the reduction of plant growth, development, and survival [5,30–35]. Indeed, sodium can reduce potassium and calcium uptake, affecting stomatal conductance; it can substitute potassium in key enzymatic reactions leading to enzyme inhibition, alteration of metabolic processes, plant nutritional imbalance and oxidative stress [23,36,37]. However, chloride can be toxic as well when accumulated in the cell at high concentrations. Nonetheless, there is a paucity of literature that documents the specific molecular and physiological mechanisms that lead to chloride adverse effects on plants [38,39].

Chloride is a micronutrient that in non-saline conditions is beneficial for plants; in fact, it accumulates to macronutrient levels through a secondary active transport, an electrogenic $Cl^-/2H^+$ symport mechanism ([40] and references therein). When present in a range of 0.2–2 $mg\ g^{-1}$ fresh weight (fw) [41,42], in addition to the well-known functions in the stabilization of the oxygen evolving complex of photosystem II (PSII), it has a key role in the maintenance of cell membranes electric potential, regulation of tonoplast H^+ -ATPase, pH-stat, amylases, and asparagine synthetase ([43] and references therein). Chloride has also been found to have adaptive functions improving water homeostasis in tobacco at concentration up to 4 $mg\ g^{-1}$ fw [44]. However, higher chloride concentration can be toxic impairing PSII quantum yield and photosynthetic electron transport rate and consequently causing other physiological dysfunctions in plants [45,46].

Taking also into account that a practice adopted in horticulture is the decrease of calcium nitrate in the culture media and its substitution with calcium chloride to meet the EU directives aimed at reducing

the accumulation of nitrate in leafy vegetables and its possible implications to human health [47]. Thus, it is of pivotal importance to understand which morphological and physiological processes are specifically impaired by chloride in excess and decrease of nitrate, and if and how the addition of OMP can alter ions/chloride homeostasis in plant tissues allowing plants to overcome the negative effects of chloride salinity. To verify this hypothesis, a greenhouse experiment was conducted to test the effect of decreasing $\text{NO}_3^-:\text{Cl}^-$ ratio in absence or presence of OMP on morpho-physiological and ion homeostasis responses of basil (*Ocimum basilicum* L.) grown in soilless culture.

2. Materials and Methods

2.1. Greenhouse Conditions, Plant Material, and Experimental Design

The trial was conducted during the growing season 2017, in a glasshouse situated at the experimental station of the Department of Agricultural Sciences, University of Naples Federico II located at Torre Lama (Bellizzi; 43°31' N, 14°58' E; 60 m above sea level). The tested crop for the present experiment was basil (*Ocimum basilicum* L., family Lamiaceae) cv. Gecom (Genovese type; Società Agricola Italiana Sementi-SAIS, Cesena, Italy). Basil plants were grown hydroponically in an open-loop soilless system using a mixture of peat and perlite as substrate. Basil seedlings were transplanted on May 9, into plastic pots containing 1.3 L of a mixture peat and perlite in a 2:1 (v:v) ratio. Plastic pots were disposed on aluminum benches (1.8 m × 8.0 m) in single row at plant density of 22 plants per square meter (15 × 30 cm). Inside the glasshouse, the daily mean temperature was maintained between 16 and 27 °C and the relative humidity ranged between 55% and 80% during the growing cycle.

Lowering the $\text{NO}_3^-:\text{Cl}^-$ ratio of the nutrient solution is a common practice in horticulture used to reduce nitrate content and improve leafy vegetables quality without altering the ionic strength of the culture media. However decreasing $\text{NO}_3^-:\text{Cl}^-$ ratio can affect the morpho-physiological and qualitative features of salt-sensitive crops. Therefore, the glasshouse experiment was designed as a factorial combination of four ratios of nitrate (NO_3^-) to chloride (Cl^-) (80:20, 60:40, 40:60, or 20:80) and two omeprazole (OMP) application levels (0 or 10 μM) to verify if OMP could ameliorate the status of plants even at very low $\text{NO}_3^-:\text{Cl}^-$ ratio. The eight treatments were arranged in a complete randomized block design, with three replicates per treatment. Each experimental unit (replication) consisted of 10 basil plants.

2.2. Nutrient Solution Management, $\text{NO}_3^-:\text{Cl}^-$ Treatments, and Omeprazole Application

The concentrations of macro (in mM) and micronutrients (in μM) in the nutrient solution were: 1.5 mM P, 4.5 mM K, 6.5 mM Ca, 2 mM Mg, 20 μM Fe, 9 μM Mn, 0.3 μM Cu, 1.6 μM Zn, 20 μM B, and 0.3 μM Mo [47]. The four $\text{NO}_3^-:\text{Cl}^-$ treatments studied in the current experiment were obtained by adding different salt quantity of calcium nitrate ($\text{Ca}[\text{NO}_3]_2$) and calcium chloride (CaCl_2) to the above nutrient solution. Particularly, the nitrate (NO_3^-), $\text{Ca}(\text{NO}_3)_2$, and CaCl_2 salt quantity in the nutrient solution were (i) 9.6 mM, 867.1 and 133.2 mg L^{-1} for 80:20 treatment, (ii) 7.2 mM, 650.3 and 266.4 mg L^{-1} for 60:40 treatment, (iii) 4.8 mM, 433.5 and 399.6 mg L^{-1} for 40:60 treatment and (iv) 2.4 mM, 216.8 and 532.8 mg L^{-1} for 20:80 treatment. The electrical conductivity (EC) and the pH of the nutrient solution in all treatments were $1.9 \pm 0.2 \text{ dS m}^{-1}$ and 6.0 ± 0.2 , respectively. The nutrient solution in the four $\text{NO}_3^-:\text{Cl}^-$ treatments were pumped from independent 50 L plastic tanks and delivered to the plants through a drip irrigation system with one auto-compensating dripper per plant having a flow rate of 2 L h^{-1} .

The OMP was supplied as root application five times during the cropping season starting on May 19 (11 days after transplanting, DAT) at seven-days interval (26 May, 2, 9, and 16 June). The OMP application was delivered manually at a uniform rate level of 100 mL per pot.

2.3. Biometric and Leaf Color Measurements

Forty-four DAT, the number of leaves per plant was recorded on six basil plants per experimental unit. Total leaf area was measured by an electronic area meter (LI-COR 3100C biosciences, Lincoln, NE, USA). Then, plants were divided in leaves, stems and roots, where the fresh yield was determined. Samples of fresh leaf, stem and root were dried at 70 °C for 72 h until they reached a constant weight, for shoot (leaves + stems) and root dry biomass assessment. The root-to-shoot ratio as well as the leaf dry matter content (%) were also calculated.

The leaf color components in particular brightness (L^*), redness (a^*) and yellowness (b^*) were also measured on the upper leaf part of six basil plants per experimental unit using an 8 mm-aperture Minolta CR-300 Chroma Meter (Minolta Camera Co. Ltd., Osaka, Japan). The calibration of the Chroma Meter was carried out just before leaf color sampling as described in detail by Colonna et al. (2016).

2.4. Soil Plant Analysis Development Index and Leaf Gas Exchange

One day before the termination of the experiment (June 20; 43 DAT), the SPAD index was measured on twenty fully developed basil leaves per replicate as described in detail by Kumar et al. [48] using a portable chlorophyll meter SPAD-502 (Konica, Minolta, Tokyo, Japan).

On the same date, all the physiological parameters including net carbon dioxide assimilation rate, stomatal resistance, transpiration rate were measured with a portable gas exchange analyzer (LCA-4; ADC BioScientific Ltd., Hoddesdon, UK) equipped with a broadleaf chamber (cuvette window area of 6.25 cm²) [49]. Similarly, to SPAD index, the leaf gas exchange measurements were carried out on fully expanded basil leaves, using six replicates per experimental unit. Instantaneous water use efficiency was calculated after dividing net CO₂ assimilation rate by transpiration rate [3].

2.5. Ion Analysis of Leaf Tissue

Total nitrogen was determined by the established Kjeldahl method [50], whereas cations and anions measurements in leaf tissue were performed according to the procedure described by Roupheal and co-workers [49] and Kyriacou et al. [51]. Total N as well as cations and anions determination were carried out on dried leaf samples, which were ground with an electrical mill to an 841 µm mesh. Briefly, two hundred fifty grams of dried leaf tissue were suspended in 50 mL of ultrapure water (Milli-Q, Merck Millipore, Darmstadt, Germany), and incubated at 80 °C for 10 min in a shaking water bath (ShakeTemp SW22, Julabo, Seelbach, Germany). The suspensions were first centrifuged (at 6000 rpm for 10 min) then filtered before injection (25 µL) in the ion chromatography (ICS-3000, Dionex, Sunnyvale, CA, USA) coupled to a conductivity detector. The implemented columns used in the current experiment were: 1) IonPac CG12A (4 250 mm, Dionex, Sunnyvale, CA, USA) guard column and IonPac CS12A (4 × 250 mm, Dionex, Sunnyvale, CA, USA) analytical column for cations (K⁺, Ca²⁺, Mg²⁺ and Na⁺) determination, 2) IonPac AG11-HC (4 × 50 mm) guard column and IonPac AS11-HC (4 × 250 mm) analytical column for anions (NO₃⁻, PO₄³⁻, SO₄²⁻, and Cl⁻) analysis.

2.6. Statistics

The experimental data were subjected to a two-way analysis of variance (ANOVA) to determine the main effects (different NO₃⁻:Cl⁻ ratios and OMP application) as well as the interaction between these two tested factors. OMP application main effects were compared by t-Test. Duncan's multiple range test was performed for mean comparisons on each of the significant ($p < 0.05$) variables measured. The software package SPSS 20 was used for the ANOVA. The Principal Component Analysis (PCA) was also conducted on morpho-physiological and mineral composition to determine the score plot and loading matrix based on the first and second principal components. The PCA analysis was assess using Minitab 16.2.1 statistical software [3,52]. The score plot and loading matrix were also determined based on the first and second principal components (PCs). A heatmap was generated using the <https://biit.cs.ut.ee/clustvis/> online program package with Euclidean distance as the similarity

measure and hierarchical clustering with complete linkage. Morpho-physiological parameters and mineral composition data were visualized using a false color scale, with red indicating an increase and blue a decrease of values [3,24]. A different heat map generated in Excel was used to summarize the plant responses to different nutrient compositions and OMP. Results were calculated as Log₂ of 60:40, 40:60, and 20:80/80:20 in control plants, and Log_{1.3} of 10 μM OMP/0 μM OMP control in plants grown at different N. Results were visualized using a false color scale with red indicating an increase and blue a decrease, while no differences were visualized by white squares [53].

3. Results

3.1. Morphological Responses Induced by OMP under Different NO₃⁻:Cl⁻ Ratios

In this experiment, for fresh yield, shoot and root dry biomass significant interactions ($p < 0.01$) were recorded between the two tested factors (NO₃⁻:Cl⁻ ratio and omeprazole [OMP] application). Fresh yield, shoot and root dry biomass were higher in OMP-treated basil plants with a varied response in terms of NO₃⁻:Cl⁻ ratio in the nutrient solution (Figure 1). In particular, basil plants treated with 10 μM OMP and grown under both 80:20 and 60:40 NO₃⁻:Cl⁻ ratio presented the highest marketable yield, shoot, and root biomass (Figure 1). Interestingly, we observed contrasting responses in treated and untreated basil plants with increasing Cl⁻ concentration in the nutrient solution (e.g., by decreasing NO₃⁻:Cl⁻ ratio). For instance, decreasing NO₃⁻:Cl⁻ ratio from 80:20 to 20:80 showed a linear reduction in the tested morphometric traits compared to the control treatment (80:20). Whereas the responses to the decrease of NO₃⁻ and simultaneous increase of Cl⁻ in conjunction to OMP diverged greatly; since no significant reduction in fresh yield, shoot and root dry biomass was observed in OMP-treated plants grown under 60:40 NO₃⁻:Cl⁻ ratio compared to the control treatment. Moreover, even in plants grown at 40:60 NO₃⁻:Cl⁻ ratio, fresh yield did not decrease compared to the control without OMP (Figure 1).

Irrespective of OMP application (no significant interaction between the two tested factors), the number of leaves, total leaf area and root-to-shoot (R/S) ratio of basil declined under the concomitant NO₃⁻ decrease and Cl⁻ increase in the nutrient solution with the lowest values observed in 20:80 NO₃⁻:Cl⁻ ratio (e.g., severe chloride conditions) (Table 1). In addition, when averaged over NO₃⁻:Cl⁻ ratio in the nutrient solution, the leaf number as well as the R/S ratio of OMP-treated basil plants were higher than those of untreated control by 14.8% and 37.5 %, respectively (Table 1).

Leaf yellow intensity expressed by positive and b* values, was significantly affected by NO₃⁻:Cl⁻ ratio and OMP treatments with no significant interaction between the two factors, whereas the leaf brightness (L*) and leaf green intensity (i.e., negative a* values) were only influenced by the ratio between NO₃⁻ and Cl⁻ when this latter was in strong favor to Cl⁻ in the nutrient solution (Table 1). Specifically, Cl⁻ concentration in the nutrient solution yielded lighter basil leaves, expressed by increasing L* values. Regardless, the NO₃⁻:Cl⁻ ratio, OMP-treated plants exhibit lower leaf yellow intensity values compared to untreated control (Table 1).

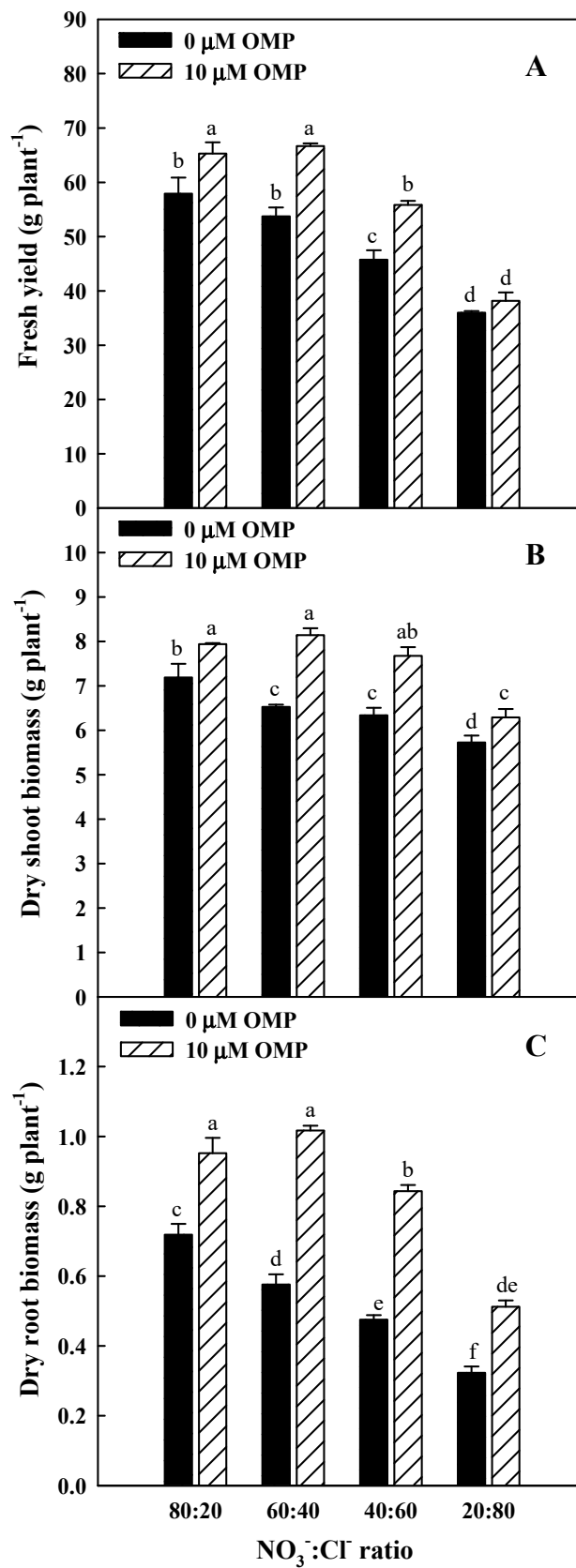


Figure 1. Effects NO₃⁻:Cl⁻ ratio in the nutrient solution and omeprazole (OMP) application rates on marketable (A) fresh yield, (B) dry shoot biomass and (C) dry root biomass of greenhouse hydroponic basil plants. Different letters indicate significant differences according to Duncan’s test (*p* = 0.05). Values are the means of three replicate samples. Vertical bars indicate ± standard error of means.

Table 1. Effects $\text{NO}_3^-:\text{Cl}^-$ ratio in the nutrient solution and omeprazole (OMP) application rates on growth parameters, root-to-shoot ratio and leaf colorimetry of greenhouse hydroponic basil plants.

| Source of variance. | Leaf Number (no. plant ⁻¹) | Leaf Area (cm ² plant ⁻¹) | Root-to-Shoot Ratio | Leaf Dry Matter (%) | L* | a* | b* |
|-------------------------------------|---|---|---------------------|------------------------|---------|-----------|---------|
| $\text{NO}_3^-:\text{Cl}^-$ (N) | | | | | | | |
| 80:20 | 103 a | 1130 a | 0.11 a | 8.73 c | 41.08 c | -15.73 a | 21.11 c |
| 60:40 | 87 b | 1196 a | 0.11 a | 8.78 c | 42.34 c | -16.20 ab | 21.20 c |
| 40:60 | 84 b | 983 b | 0.09 b | 9.56 b | 44.40 b | -16.92 b | 23.14 b |
| 20:80 | 73 c | 751 c | 0.07 c | 11.18 a | 46.49 a | -18.19 c | 25.87 a |
| | *** | *** | *** | *** | *** | *** | *** |
| Omeprazole (μM) (OMP) | | | | | | | |
| 0 | 81 | 955 | 0.08 | 9.62 | 43.66 | -17.13 | 24.03 |
| 10 | 93 | 1076 | 0.11 | 9.51 | 43.49 | -16.39 | 21.62 |
| t-test | 0.030 | 0.150 | 0.001 | 0.832 | 0.876 | 0.125 | 0.021 |
| N \times OMP | | | | | | | |
| 80:20 \times 0 μM OMP | 98 | 1123 | 0.10 | 9.16 | 41.98 | -16.42 | 22.04 |
| 60:40 \times 0 μM OMP | 78 | 1124 | 0.09 | 8.71 | 42.19 | -16.55 | 21.64 |
| 40:60 \times 0 μM OMP | 77 | 895 | 0.08 | 9.66 | 44.22 | -17.20 | 24.72 |
| 20:80 \times 0 μM OMP | 71 | 678 | 0.06 | 10.93 | 46.25 | -18.35 | 27.74 |
| 80:20 \times 10 μM OMP | 109 | 1138 | 0.12 | 8.31 | 40.19 | -15.03 | 20.18 |
| 60:40 \times 10 μM OMP | 95 | 1268 | 0.13 | 8.86 | 42.48 | -15.85 | 20.76 |
| 40:60 \times 10 μM OMP | 91 | 1072 | 0.11 | 9.46 | 44.57 | -16.63 | 21.55 |
| 20:80 \times 10 μM OMP | 75 | 825 | 0.08 | 11.42 | 46.73 | -18.03 | 24.01 |
| | ns | ns | ns | ns | ns | ns | ns |

ns, *** not significant or significant at $p \leq 0.001$, respectively. Different letters within each column indicate significant differences according to Duncan's multiple-range test ($p = 0.05$). Omeprazole application rates are compared according to Student's t-test.

3.2. Physiological Responses Induced by OMP under Different $\text{NO}_3^-:\text{Cl}^-$ Ratios

SPAD index and leaf gas exchange as a function of $\text{NO}_3^-:\text{Cl}^-$ ratio and OMP application are reported in Table 2. No significant interaction between the two tested factors were observed in the studied physiological parameters. When averaged over OMP application, increasing the Cl^- concentration in the nutrient solution reduced linearly the SPAD index and net CO_2 assimilation rate (A_{CO_2}) as well as the transpiration rate (E), while it increased the stomatal resistance (r_s) (Table 2). Moreover, irrespective $\text{NO}_3^-:\text{Cl}^-$ ratio, substrate drench application of 10 μM OMP increased A_{CO_2} and instantaneous water use efficiency (WUE_i) and decrease r_s by 13.9%, 27.2%, and 18.4%, respectively compared to untreated soilless basil plants (Table 2).

3.3. Ion Content Induced by OMP under Different $\text{NO}_3^-:\text{Cl}^-$ Ratios

Neither $\text{NO}_3^-:\text{Cl}^-$ ratio nor substrate drench OMP application had a significant effect on Na^+ concentration (avg. 0.17 g kg^{-1} dry weight; dw) in leaf tissue (data not shown). Our results demonstrated that NO_3^- , PO_4^{3-} , SO_4^{2-} , and Cl^- were highly influenced by the interaction $\text{NO}_3^-:\text{Cl}^-$ ratio \times OMP, whereas total N, monovalent (K^+) and bivalent (Ca^{2+}) cations were only affected by the lowest $\text{NO}_3^-:\text{Cl}^-$ ratio (Table 3). The N concentration in leaves decreased linearly with increasing Cl^- in the nutrient solution, whereas the detrimental effect of chloride salinity on K^+ and Ca^{2+} was only observed under severe chloride concentration (20:80 treatment; Table 3). Concerning the nitrate, phosphate and sulphate concentration a $\text{NO}_3^-:\text{Cl}^-$ ratio-dependent response to OMP application was observed with NO_3^- , PO_4^{3-} , and SO_4^{2-} concentration being the highest in OMP-treated plants grown at 80:20 (for nitrate) and at both 80:20 and 60:40 ratios (for phosphate and sulphate) (Table 3). Interestingly, the substrate drench application of 10 μM OMP effectively reduced the toxic anion (Cl^-) accumulation in leaf tissue under Cl^- stress conditions (60:40, 40:60 and 20:80 NO_3^- , PO_4^{3-} , SO_4^{2-} ratios) but not under control conditions (80:20 NO_3^- , PO_4^{3-} , SO_4^{2-} ratio; Table 3). Under Cl^- stress conditions OMP-treated basil plants significantly reduced the accumulation of Cl^- in the aerial part in a dose-dependent manner: -40.5% , -36.9% , and -24.0% in response to 60:40, 40:60, and 20:80 $\text{NO}_3^-:\text{Cl}^-$ ratio, respectively (Table 3).

Table 2. Effects $\text{NO}_3^-:\text{Cl}^-$ ratio in the nutrient solution and omeprazole (OMP) application rates on physiological parameters: SPAD index, net CO_2 assimilation (A_{CO_2}), stomatal resistance (r_s), transpiration rate (E) and instantaneous water use efficiency (WUE_i) of greenhouse hydroponic basil plants.

| Source of Variance | SPAD Index | A_{CO_2} ($\mu\text{mol CO}_2 \text{ m}^{-2} \text{ s}^{-1}$) | r_s ($\text{m}^{-2} \text{ s}^{-1} \text{ mol}^{-1}$) | E ($\text{mol H}_2\text{O m}^{-2} \text{ s}^{-1}$) | WUE_i ($\mu\text{mol CO}_2 \text{ mol}^{-1} \text{ H}_2\text{O}$) |
|-------------------------------------|------------|---|--|---|---|
| $\text{NO}_3^-:\text{Cl}^-$ (N) | | | | | |
| 80:20 | 39.59 a | 11.89 a | 5.56 b | 3.81 a | 3.16 |
| 60:40 | 38.35 ab | 11.67 ab | 8.01 a | 3.29 ab | 3.60 |
| 40:60 | 37.25 b | 10.60 bc | 7.52 ab | 3.09 b | 3.48 |
| 20:80 | 31.59 c | 9.57 c | 8.35 a | 2.96 b | 3.32 |
| | *** | ** | * | * | ns |
| Omeprazole (μM) (OMP) | | | | | |
| 0 | 35.64 | 10.22 | 8.10 | 3.45 | 2.98 |
| 10 | 37.74 | 11.64 | 6.61 | 3.13 | 3.79 |
| t-test | 0.145 | 0.014 | 0.050 | 0.126 | 0.001 |
| N \times OMP | | | | | |
| 80:20 \times 0 μM OMP | 38.27 | 11.71 | 6.34 | 4.03 | 2.92 |
| 60:40 \times 0 μM OMP | 37.04 | 11.02 | 8.41 | 3.38 | 3.29 |
| 40:60 \times 0 μM OMP | 36.47 | 9.87 | 8.10 | 3.22 | 3.09 |
| 20:80 \times 0 μM OMP | 30.79 | 8.29 | 9.56 | 3.16 | 2.63 |
| 80:20 \times 10 μM OMP | 40.90 | 12.06 | 4.78 | 3.59 | 3.41 |
| 60:40 \times 10 μM OMP | 39.65 | 12.32 | 7.60 | 3.20 | 3.90 |
| 40:60 \times 10 μM OMP | 38.04 | 11.33 | 6.93 | 2.97 | 3.87 |
| 20:80 \times 10 μM OMP | 32.38 | 10.86 | 7.14 | 2.75 | 4.00 |
| | ns | ns | ns | ns | ns |

ns, *, **, *** not significant or significant at $p \leq 0.05$, 0.01 or 0.001, respectively. Different letters within each column indicate significant differences according to Duncan's multiple-range test ($p = 0.05$). Omeprazole application rates are compared according to Student's t-test.

Table 3. Effects $\text{NO}_3^-:\text{Cl}^-$ ratio in the nutrient solution and omeprazole (OMP) application rates on total nitrogen (N), nitrate (NO_3^-), phosphate (PO_4^{3-}), sulphate (SO_4^{2-}), potassium (K^+), calcium (Ca^{2+}), magnesium (Mg^{2+}), chloride (Cl^-).

| Source of Variance | Total N (g 100 g ⁻¹ DW) | NO_3^- (g kg ⁻¹ DW) | PO_4^{3-} (g kg ⁻¹ DW) | SO_4^{2-} (g kg ⁻¹ DW) | K^+ (g kg ⁻¹ DW) | Ca^{2+} (g kg ⁻¹ DW) | Mg^{2+} (g kg ⁻¹ DW) | Cl^- (g kg ⁻¹ DW) |
|------------------------------------|---------------------------------------|--|---|---|---|---|---|--|
| $\text{NO}_3^-:\text{Cl}^-$ (N) | | | | | | | | |
| 80:20 | 4.40 a | 29.09 a | 33.13 a | 3.68 a | 54.16 a | 11.55 a | 2.41 ab | 5.31 d |
| 60:40 | 4.05 b | 19.82 b | 29.78 b | 3.30 ab | 54.53 a | 11.57 a | 2.52 a | 13.21 c |
| 40:60 | 3.16 c | 6.69 c | 21.77 c | 2.93 b | 54.92 a | 12.37 a | 2.29 b | 26.58 b |
| 20:80 | 2.19 d | 0.92 d | 13.66 d | 2.35 c | 43.26 b | 10.15 b | 2.39 ab | 36.80 a |
| | *** | *** | *** | *** | *** | ** | ns | *** |
| Omeprazole (μM) (OMP) | | | | | | | | |
| 0 | 3.37 | 11.76 | 19.86 | 2.50 | 43.50 | 10.34 | 2.07 | 24.44 |
| 10 | 3.53 | 16.51 | 29.31 | 3.63 | 59.93 | 12.48 | 2.74 | 16.51 |
| t-test | 0.674 | 0.339 | 0.012 | 0.001 | 0.001 | 0.001 | 0.001 | 0.048 |
| N × O | | | | | | | | |
| 80:20 × 0 μM OMP | 4.34 | 24.34 b | 26.03 b | 2.86 bc | 44.59 | 10.28 | 2.02 | 6.73 de |
| 60:40 × 0 μM OMP | 4.03 | 15.56 c | 23.25 bc | 2.51 cd | 44.37 | 10.76 | 2.22 | 16.57 c |
| 40:60 × 0 μM OMP | 3.12 | 6.13 d | 18.85 cd | 2.53 cd | 47.95 | 11.00 | 1.98 | 32.61 b |
| 20:80 × 0 μM OMP | 2.02 | 0.99 e | 11.31 e | 2.10 d | 37.10 | 9.32 | 2.04 | 41.85 a |
| 80:20 × 10 μM OMP | 4.47 | 33.84 a | 40.23 a | 4.50 a | 63.74 | 12.82 | 2.80 | 3.90 e |
| 60:40 × 10 μM OMP | 4.08 | 24.08 b | 36.31 a | 4.08 a | 64.68 | 12.38 | 2.81 | 9.85 d |
| 40:60 × 10 μM OMP | 3.21 | 7.26 d | 24.70 b | 3.33 b | 61.88 | 13.75 | 2.60 | 20.55 c |
| 20:80 × 10 μM OMP | 2.37 | 0.85 e | 16.00 d | 2.60 cd | 49.42 | 10.97 | 2.74 | 31.75 b |
| | ns | ** | * | * | ns | ns | ns | * |

ns, *, **, *** not significant or significant at $p \leq 0.05$, 0.01 or 0.001, respectively. Different letters within each column indicate significant differences according to Duncan's multiple-range test ($p = 0.05$). Omeprazole application rates are compared according to Student's t-test.

3.4. Heat Map Analysis

The aggregated data heat-map analysis (Figure 2) identified two main clusters corresponding to the 20:80 × 10 μM OMP and 20:80 and 40:60 without OMP on the left and all the other treatments on the right. This indicated that the $\text{NO}_3^-:\text{Cl}^-$ ratio of nutrient solution was the main clustering factor responsible for different effects. Indeed, two separated sub-clusters could be defined under both the first and the second clusters which illustrated the $\text{NO}_3^-:\text{Cl}^-$ ratio × OMP interaction. In particular, the OMP application at 20:80 ratio subcluster separated from that with 20:80 and 40:60 ratios without OMP because of the higher WUEi and Mg^{2+} (in common with all other OMP Treatments), lower E, but higher A_{CO_2} . While 80:20 and 60:40 ratios without OMP separated from 80:20, 60:40, and 40:60 ones plus OMP because of their higher dry shoot and root biomass, K^+ and Ca^{2+} . In particular, 80:20 and 60:40 $\text{NO}_3^-:\text{Cl}^-$ ratios plus OMP showed the highest A_{CO_2} , a^* , PO_4^{3-} , SO_4^{2-} , SPAD index, fresh yield and leaf number. These latter treatments showed also in common with the treatment 80:20 ratio without OMP the highest total N, NO_3^- , and LN, but the lowest Cl^- content. On the other hand, the 20:80 treatment without OMP showed the lowest A_{CO_2} , LA, SPAD, dry shoot and root biomass, K^+ , Ca^{2+} , and WUEi (Figure 2).

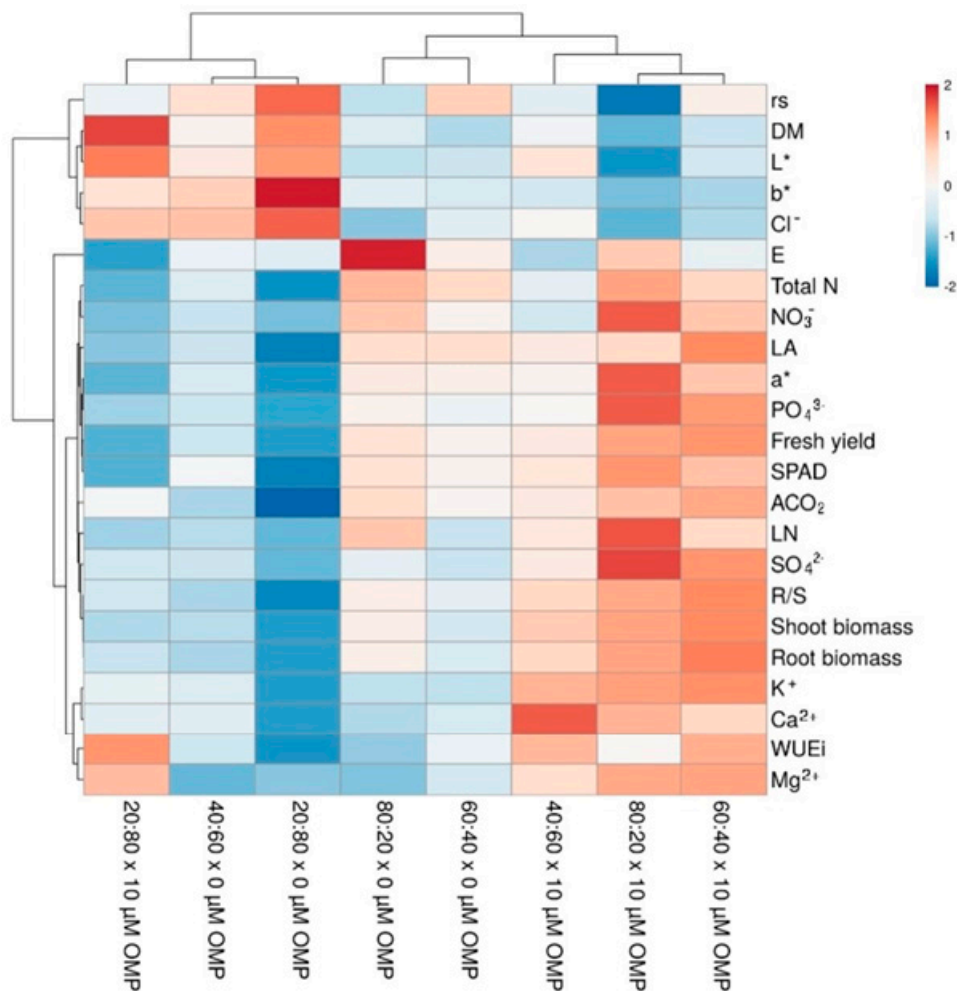


Figure 2. Cluster heat map analysis summarizing plant responses to drench application of (0 μM and 10 μM OMP) and different $\text{NO}_3^-:\text{Cl}^-$ ratios in the nutrient solution (80:20, 60:40, 40:60, and 20:80). It was generated using the <https://biit.cs.ut.ee/clustvis/> online program package with Euclidean distance as the similarity measure and hierarchical clustering with complete linkage.

A different heat map analysis evaluating the changes in the analyzed parameters in dependence on the $\text{NO}_3^-:\text{Cl}^-$ ratios in the nutrient solution (Figure 3A) and OMP application (Figure 3B) separately was also performed. The decrease of $\text{NO}_3^-:\text{Cl}^-$ ratio compared to the highest N ratio, showed a clear increase of Cl^- , b^* , L^* , and r_s and a decrease of NO_3^- , total N, fresh yield, leaf area (LA), leaf number (LN), PO_4^{3-} , root-to-shoot (R/S) ratio, dry shoot and root biomass, and SO_4^{2-} . However, OMP application improved dry root biomass, R/S, PO_4^{3-} , Mg^{2+} , K^+ compared to all the respective controls, while Cl^- decreased, even if not significantly at 80:20 ratio. Only at 80:20 and 60:40 N, OMP increased NO_3^- and SO_4^{2-} , while total N decreased. Finally, OMP application increased WUE_i and A_{CO_2} but only at 20:80 ratio.

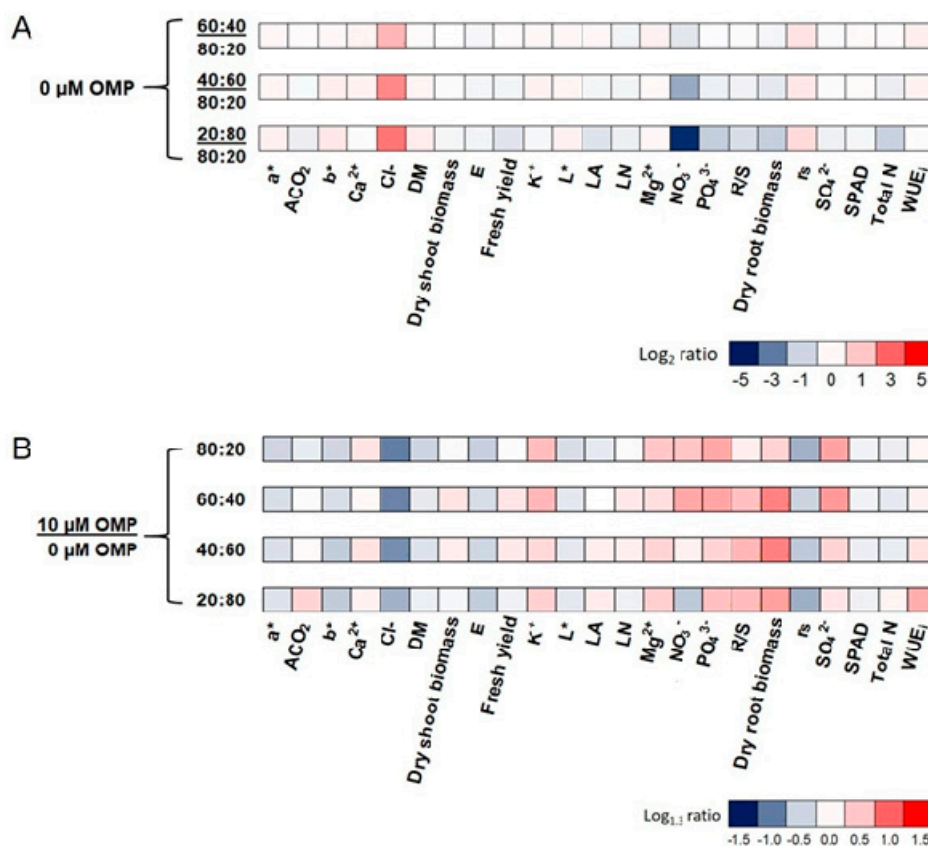


Figure 3. Heat map analysis summarizing the plant response to different $\text{NO}_3^-:\text{Cl}^-$ ratios (80:20, 60:40, 40:60, and 20:80) and OMP treatments. Results were calculated as Logarithm base 2 (Log_2) of 60:40, 40:60, and 20:80/80:20 in control plants (A) or Logarithm base 1.3 ($\text{Log}_{1.3}$) of 10 μM OMP/0 μM OMP control in plants grown at different N (B) and visualized using a false color scale with red indicating an increase and blue a decrease. No differences were visualized by white squares.

3.5. Principal Component Analysis

The score plot and loading matrix based on the first and second principal components PC1 and PC2 are reported in Figure 4. The first two PCs were associated with eigen values higher than 1 and explained 90.7% of the cumulative variance, with PC1 and PC2 accounting for 74.9% and 15.8%, respectively (data not shown). PC1 was strongly and positively correlated to morphometric traits (leaf number and area, fresh yield, shoot and root biomass, and R/S ratio), SPAD index and A_{CO_2} as well as the ion content in leaf tissue (N, NO_3^- , PO_4^{3-} , SO_4^{2-} , K^+ , and Ca^{2+}); and negatively correlated with leaf color parameters (L^* and b^*), leaf dry matter percentage, Cl^- concentration and r_s . In addition, PC2 was positively associated with Mg^{2+} and WUE_i and negatively correlated with transpiration rate (E). Furthermore, based on the loading matrix, our PCA indicated that variation in above and

below ground biomass were most closely aligned with A_{CO_2} , while variation in nitrate content was not correlated to leaf dry matter (DM) percentage (Figure 4).

Moreover, the score plot derived from the PCA clearly divided the OMP application along PC2 with substrate drench OMP-treated plants (except for 80:20 $NO_3^-:Cl^-$ ratio) on the positive side of the second PCs. For instance, basil plants treated with 10 μM OMP were characterized by improved SPAD index and fresh yield (at 80:20 $NO_3^-:Cl^-$ ratio) and higher shoot and root biomass, nutritional, physiological status, and photosynthetic performance (at 60:40 and 40:60 $NO_3^-:Cl^-$ ratio). Finally, the untreated basil plants especially those grown under moderate to severe Cl^- stress in the nutrient solution (40:60 and 20:80 $NO_3^-:Cl^-$ ratio) were characterized by the lowest agronomic performance due to the high stomatal resistance and accumulation of toxic ions (Cl^-) in leaf tissue (Figure 4).

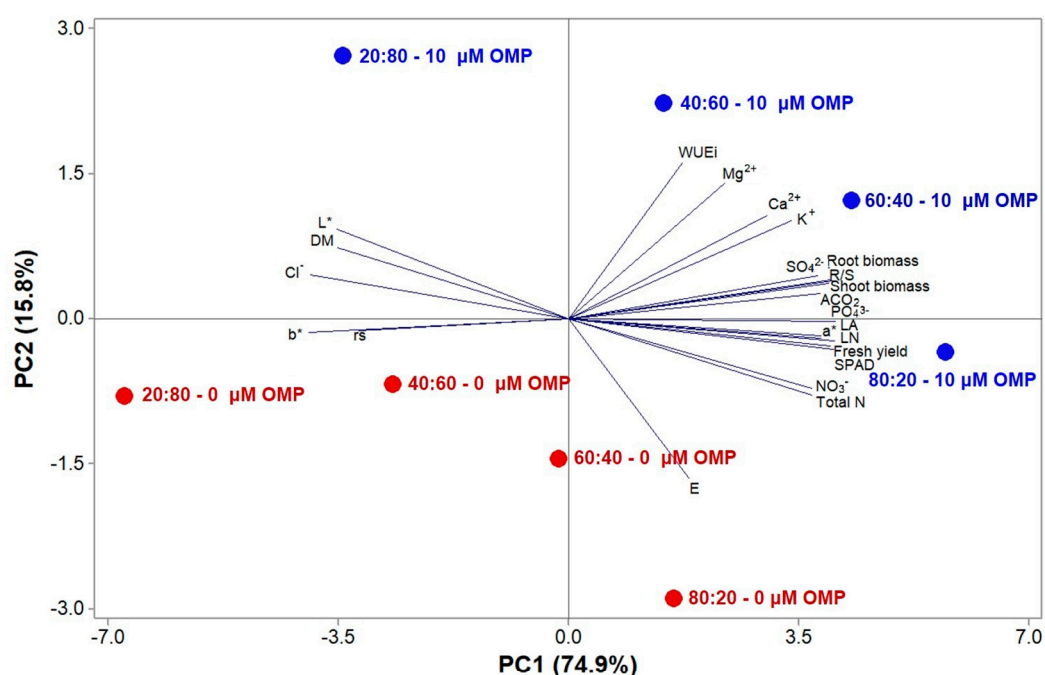


Figure 4. Principal component loading plot and scores of principal component analysis (PCA) of growth parameters, fresh yield, shoot and root dry biomass, leaf dry matter (leaf DM), leaf area (LA) and leaf number (LN), WUE_i , total N, mineral concentrations, net CO_2 assimilation rate (A_{CO_2}), SPAD index, a^* , b^* , and L^* , in untreated (0 μM OMP) and treated greenhouse basil plants with 10 μM OMP grown under different $NO_3^-:Cl^-$ ratios (80:20, 60:40, 40:60, and 20:80).

4. Discussion

Herbaceous species can be more sensitive to chloride than sodium, with critical levels of chloride varying between 4 and 7 $mg\ g^{-1}$ fresh weight (FW) [54]. Mild to moderate concentrations of $CaCl_2$ can induce ion imbalance and hyperosmotic stress even more severe than $NaCl$ in different horticultural species, reducing plant growth and yield [55–57]. This was demonstrated in the present experiment in which basil plants were submitted to a factorial combination of four ratios of nitrate (NO_3^-) to chloride (Cl^-) (80:20, 60:40, 40:60, or 20:80).

Significant decrease in morphological traits (e.g., number of leaves, total leaf area and R/S ratio) was noted under severe chloride treatment (20:80 $NO_3^-:Cl^-$ ratio), which, in turn, reduced the fresh yield. Stomatal resistance (r_s) of basil plants increased with the decrease of $NO_3^-:Cl^-$ ratio in the nutrient solution while transpiration (E) was linearly reduced, affecting net CO_2 assimilation rate (A_{CO_2}). Accordingly, Geilfus and co-workers [39] proved that the exposure of *Vicia faba* plant roots to high Cl^- levels could induce a long-distance signal causing leaf apoplastic pH alkalinization, leaf ABA redistribution, stomata closure, and therefore an indirect inhibition of photosynthesis.

NO_3^- , PO_4^{3-} , and SO_4^{2-} were severely reduced by the decrease of $\text{NO}_3^-:\text{Cl}^-$ ratio while Cl^- strongly increased. Chloride uses the same anion channels used by nitrate [58], specifically interfering with nitrate uptake, transport and loading in the root xylem [59]. This implies that nitrate transport to leaves decreases, while excess chloride increases being also less controlled compared to that of sodium [1,56].

To further worsen the chloride salinity impact, there is the lower capacity to exclude chloride than sodium from the leaf blades [1] and the scarce basipetal re-translocation of this ion from leaves to roots via the phloem compared to that of sodium [39,60]. The chloride-dependent reduction of nitrate levels in the cells can indirectly downregulate nitrate uptake by lowering nitrate internal demand [61]. In fact, nitrate in the cell induces the expression and the transcription of genes involved in nitrate assimilation and transport, including high affinity nitrate transporters and nitrate reductase genes, in addition to genes involved in energy and carbon metabolism [62–64]. Moreover, nitrate deficiency indirectly accelerates yellowing and senescence of older leaves, since it induces proteolysis of plastidial proteins and amino acid remobilization to young leaves ([65] and references therein). Accordingly, the increase of chloride in basil leaves caused a decrease of photosynthetic pigments as proved by the decrease of the SPAD index and a lighter color of basil leaves (higher L^*).

The negative effects of chloride were mitigated by the application of OMP, with a lower beneficial effect of OMP in the treatment 20:80 $\text{NO}_3^-:\text{Cl}^-$ ratio. In particular, plants growth at 80:20 and 60:40 $\text{NO}_3^-:\text{Cl}^-$ ratios and treated with OMP showed the highest fresh yield, shoot and root biomass; while those grown with 40:60 $\text{NO}_3^-:\text{Cl}^-$ ratio and treated with 10 μM OMP did not show a decrease of fresh yield compared to the control without OMP. OMP also determined an increase of the root to shoot ratio (R/S) which is supposed to be a trait of salt tolerance [66].

The treatments with OMP, with the exception of that at 20:80 $\text{NO}_3^-:\text{Cl}^-$ ratio, kept unchanged the leaf area and number and increased and/or preserved SPAD index, A_{CO_2} and instantaneous water use efficiency (WUE_i) at levels comparable to those of 80:20 ratio without OMP while decreasing r_s . Probably OMP was able to preserve photosynthetic apparatus and transpiration processes because of the higher nitrate and potassium content, and lower chloride concentration present in basil leaves at 80:20, 60:40, and 40:60 $\text{NO}_3^-:\text{Cl}^-$ ratios. Cirillo and co-workers [25], by using OMP to ameliorate salinity toxicity in the salt sensitive basil genotype Napoletano, ascribed the beneficial effect of this small bioactive molecule to the higher acquired capacity to exclude chloride from the cytosol of salt stressed cells. However, OMP more than increasing the ability of plant to better compartmentalize chloride in vacuole or exclude it in the apoplast of basil leaf cells, is able to limit the access of chloride to the above ground parts of the plant, as inferred by the lower Cl^- content in the leaf in all the $\text{NO}_3^-:\text{Cl}^-$ treatments with the exception of the 20:80 one. Chloride exclusion is considered the main mechanism contributing to salt tolerance in soybean [67], while, on the contrary, its accumulation in soybean leaves is correlated with decreased transpiration and photosynthesis, reduced crop quality and yield, and finally plant death ([68] and references therein).

The key step of chloride transport and accumulation in the shoot, which antagonizes the nitrate transfer to the shoot, is the loading of chloride from the root stelar symplast to xylem apoplast, which is regulated/inhibited by the stress-induced abscisic acid (ABA) and cytosolic Ca^{2+} [68,69]. As suggested by Rouphael et al. [23] in tomato plants treated with OMP, this small bioactive molecule can trigger signal transduction pathways mediated by endogenous phytohormones or calcium, or in this case induce the synthesis of hormones (i.e., ABA), which can activate sub-traits that confer chloride salinity tolerance.

ABA has no effect on chloride uptake by roots or its compartmentalization in root vacuole ([68] and references therein). However, *AtNPF2.5*, a homolog of *AtNPF2.4* belonging to the root nitrate excretion transporter subfamily (NAXT) localized to the plasma membrane of root cortical cells, has been suggested to encode a transporter which mediates Cl^- excretion from the roots under salinity and is also able to transport ABA [70]. OMP could be therefore involved in the regulation of the

expression of this NAXT type gene exerting an action of chloride extrusion from root cells in presence of ABA.

Moreover, it has been proved in *Arabidopsis* that a single missense mutation in CLCa, a member of the family of anion transporters CLC implicated in the vacuolar storage of NO_3^- , can change the selectivity of the channel from NO_3^- to Cl^- determining the Cl^- compartmentalization in the root vacuoles and consequent lower loading to leaves [71]. OMP could be also involved in this kind of specific epigenetic modification implying the compartmentalization of chloride into vacuoles of root cells thus improving basil tolerance to salinity.

Whatever the reason for reducing the loading of Cl^- to shoot, this generates an increase of NO_3^- and even more of potassium in the leaves. An outwardly rectifying non-selective cation channel (NORC) identified in barley roots xylem parenchyma cells by Wegner and Raschke [72] could be responsible for this phenomenon. The channel, activated by membrane depolarization, possibly due to active Cl^- extrusion or compartmentalization in the vacuole, is permeable to the Cl^- and NO_3^- but about twice more is permeable to cations [73]. This channel could be responsible for the simultaneous passive non-selective transport/loading of NO_3^- and K^+ to shoot. This could also explain the higher K^+ content in OMP treated plants than 80:20 ratio without OMP, responsible for the increase in leaf area/expansion and fresh yield. Finally, OMP was no more able to exert a positive effect on basil tolerance to Cl^- when very severe Cl^- conditions were applied, 20:80 $\text{NO}_3^-:\text{Cl}^-$ ratio.

5. Conclusions

Chloride toxicity, that is exerted at relatively low concentrations starting from 4–7 mg g^{-1} in glycophytes, can be more dangerous than sodium because its transport is less controlled. Notwithstanding, the study of chloride salinity has been almost neglected compared to that of sodium. OMP seems responsible for control of chloride transport and exclusion from shoots improving salt tolerance in basil. The fact that it limits chloride loading to shoot while favoring those of nitrate, potassium, and other beneficial ions, boosts photosynthetic activity and leaf metabolism determining a significant increase in leaf expansion and marketable fresh yield. The mechanisms by which OMP can control/reduce chloride loading to shoot certainly require further molecular study in particular about chloride transporter/excluder channels. However, it is clear that OMP use is absolutely beneficial to plants, and can be useful to unravel the molecular mechanisms involved in chloride salt tolerance.

Author Contributions: Conceptualization, Y.R. and G.R.; methodology, Y.R.; software, P.C. and A.P.; validation, Y.R., P.C., C.E.N., A.P., and M.G.; resources, P.C. and P.W.; C.E.N., A.P., M.G., and M.M.; writing—original draft preparation, P.C. and Y.R.; writing—review and editing, P.C., M.C.K., G.C., S.D.P., and Y.R.; visualization, P.C. and Y.R.; supervision, Y.R.; project administration, Y.R. and G.R.; funding acquisition, P.C. and P.W.

Funding: This research received no external funding.

Conflicts of Interest: The authors declare no conflict of interest.

References

1. Munns, R.; Tester, M. Mechanisms of salinity tolerance. *Ann. Rev. Plant Biol.* **2008**, *59*, 651–681. [[CrossRef](#)] [[PubMed](#)]
2. Shabala, S.; Munns, R. Salinity stress: Physiological constraints and adaptive mechanisms. *Plant Stress Physiol.* **2012**, *1*, 59–63. [[CrossRef](#)]
3. Carillo, P.; Cirillo, C.; De Micco, V.; Arena, C.; De Pascale, S.; Roupael, Y. Morpho-anatomical; physiological and biochemical adaptive responses to saline water of *Bougainvillea spectabilis* Willd. trained to different canopy shapes. *Agric. Water Manag.* **2019**, *212*, 12–22. [[CrossRef](#)]
4. Hasegawa, P.M.; Bressan, R.A.; Zhu, J.K.; d Bohnert, H.J. Plant cellular and molecular responses to high salinity. *Annu. Rev. Plant Physiol Plant. Mol. Biol.* **2000**, *51*, 463–499. [[CrossRef](#)] [[PubMed](#)]
5. Flowers, T.J.; Munns, R.; Colmer, T.D. Sodium chloride toxicity and the cellular basis of salt tolerance in halophytes. *Ann. Bot.* **2015**, *115*, 419–431. [[CrossRef](#)] [[PubMed](#)]

6. Scagel, C.F.; Bryla, D.R.; Lee, J. Salt Exclusion and mycorrhizal symbiosis increase tolerance to NaCl and CaCl₂ salinity in 'Siam Queen' basil. *HortScience* **2017**, *52*, 278–287. [[CrossRef](#)]
7. Ferchichi, S.; Hessini, K.; Dell'Aversana, E.; D'Amelia, L.; Woodrow, P.; Ciarmiello, L.F.; Fuggi, A.; Carillo, P. *Hordeum vulgare* and *Hordeum maritimum* respond to extended salinity stress displaying different temporal accumulation pattern of metabolites. *Funct. Plant Biol.* **2018**, *45*, 1096–1109. [[CrossRef](#)]
8. Gorham, J.; Läuchli, A.; Leidi, E.O. Plant Responses to Salinity. In *Physiology of Cotton*; Stewart, J.M., Oosterhuis, D.M., Heitholt, J.J., Mauney, J.R., Eds.; Springer: Dordrecht, The Netherlands, 2010; pp. 129–141.
9. Annunziata, M.G.; Ciarmiello, L.F.; Woodrow, P.; Dell'Aversana, E.; Carillo, P. Spatial and temporal profile of glycine betaine accumulation in plants under abiotic stresses. *Front. Plant Sci.* **2019**, *10*. [[CrossRef](#)]
10. FAO. *Small-Scale Irrigation for Arid Zones. Principles and Options*; FAO, Development Series 2; Food and Agriculture Organisation of the United Nations, FAO: Rome, Italy, 1997; p. 51. ISBN 97892 51038 963.
11. Chinnusamy, V.; Jagendorf, A.; Zhu, J.K. Understanding and improving salt tolerance in plants. *Crop Sci.* **2005**, *45*, 437–448. [[CrossRef](#)]
12. Negrão, S.; Schmöckel, S.M.; Tester, M. Evaluating physiological responses of plants to salinity stress. *Ann. Bot.* **2017**, *119*, 1–11. [[CrossRef](#)]
13. Puniran-Hartley, N.; Hartley, J.; Shabala, L.; Shabala, S. Salinity-induced accumulation of organic osmolytes in barley and wheat leaves correlates with increased oxidative stress tolerance: In planta evidence for cross-tolerance. *Plant Physiol. Biochem.* **2014**, *83*, 32–39. [[CrossRef](#)] [[PubMed](#)]
14. Kumar, D.; Al Hassan, M.; Naranjo, M.A.; Agrawal, V.; Boscaiu, M.; Vicente, O. Effects of salinity and drought on growth; ionic relations; compatible solutes and activation of antioxidant systems in oleander (*Nerium oleander* L.). *PLoS ONE* **2017**, *12*, e0185017. [[CrossRef](#)] [[PubMed](#)]
15. Mansour, M.M.F. Nitrogen containing compounds and adaptation of plants to salinity stress. *Biol. Plant.* **2000**, *43*, 491–500. [[CrossRef](#)]
16. Yancey, P.H. Organic osmolytes as compatible; metabolic and counteracting cytoprotectants in high osmolarity and other stresses. *J. Exp. Biol.* **2005**, *208*, 2819–2830. [[CrossRef](#)] [[PubMed](#)]
17. Carillo, P. GABA shunt in durum wheat. *Front. Plant Sci.* **2018**, *9*. [[CrossRef](#)] [[PubMed](#)]
18. Kaschani, F.; van der Hoorn, R. Small molecule approaches in plants. *Curr. Opin. Chem. Biol.* **2007**, *11*, 88–98. [[CrossRef](#)] [[PubMed](#)]
19. Hicks, G.R.; Raikhel, N.V. Small molecules present large opportunities in plant biology. *Ann. Rev. Plant Biol.* **2012**, *63*, 261–282. [[CrossRef](#)]
20. Chan, Z.; Shi, H. Improved abiotic stress tolerance of bermudagrass by exogenous small molecules. *Plant Signal. Behav.* **2015**, *10*, e991577. [[CrossRef](#)]
21. Lace, B.; Prandi, C. Shaping small bioactive molecules to untangle their biological function: A focus on fluorescent plant hormones. *Mol. Plant* **2016**, *9*, 1099–1118. [[CrossRef](#)]
22. Van Oosten, M.J.; Silletti, S.; Guida, G.; Cirillo, V.; Di Stasio, E.; Carillo, P.; Woodrow, P.; Maggio, A.; Raimondi, G. A benzimidazole proton pump inhibitor increases growth and tolerance to salt stress in tomato. *Front. Plant Sci.* **2017**, *8*, 1220. [[CrossRef](#)]
23. Roupheal, Y.; Raimondi, G.; Lucini, L.; Carillo, P.; Kyriacou, M.C.; Colla, G.; Cirillo, V.; Pannico, A.; El-Nakhel, C.; De Pascale, S. Physiological and metabolic responses triggered by omeprazole improve tomato plant tolerance to NaCl stress. *Front. Plant Sci.* **2018**, *9*, 249. [[CrossRef](#)] [[PubMed](#)]
24. Carillo, P.; Raimondi, G.; Kyriacou, M.C.; Pannico, A.; El-Nakhel, C.; Cirillo, V.; Colla, G.; De Pascale, S.; Roupheal, Y. Morpho-physiological and homeostatic adaptive responses triggered by omeprazole enhance lettuce tolerance to salt stress. *Sci. Hortic.* **2019**, *249*, 22–30. [[CrossRef](#)]
25. Cirillo, V.; Van Oosten, M.J.; Izzo, M.; Maggio, A. Omeprazole treatment elicits contrasting responses to salt stress in two basil genotypes. *Ann. Appl. Biol.* **2019**, 1–10. [[CrossRef](#)]
26. Okamoto, T.; Takatani, S.; Noutoshi, Y.; Motose, H.; Takahashi, T. Omeprazole enhances mechanical stress-induced root growth reduction in *Arabidopsis thaliana*. *Plant Cell Physiol.* **2018**, *59*, 1581–1591. [[CrossRef](#)] [[PubMed](#)]
27. Fellenius, E.; Berglindh, T.; Sachs, G.; Olbe, L.; Elander, B.; Sjöstrand, S.E.; Wallmark, B. Substituted benzimidazoles inhibit gastric acid secretion by blocking (H⁺ + K⁺) ATPase. *Nature* **1981**, *290*, 159–161. [[CrossRef](#)] [[PubMed](#)]

28. Clissold, S.; Campoli-Richards, D. Omeprazole. A preliminary review of its pharmacodynamic and pharmacokinetic properties; and therapeutic potential in peptic ulcer disease and Zollinger-Ellison syndrome. *Drugs* **1986**, *32*, 15–47. [[CrossRef](#)] [[PubMed](#)]
29. Massoomi, F.; Savage, J.; Destache, C.J. Omeprazole: A comprehensive review. *Pharmacother. J. Hum. Pharmacol. Drug Ther.* **1993**, *13*, 46–59. [[CrossRef](#)]
30. Blumwald, E. Sodium transport and salt tolerance in plants. *Curr. Opin. Cell Biol.* **2000**, *12*. [[CrossRef](#)]
31. Pardo, J.M.; Quintero, F.J. Plants and sodium ions: Keeping company with the enemy. *Genome Biol.* **2002**, *3*, REVIEWS1017. [[CrossRef](#)]
32. Munns, R.; Rebetzke, G.J.; Husain, S.; James, R.A.; Hare, R.A. Genetic control of sodium exclusion in durum wheat. *Aust. J. Agric. Res.* **2003**, *54*, 627–635. [[CrossRef](#)]
33. Davenport, R.; James, R.; Zakrisson-Plogander, A.; Tester, M.; Munns, R. Control of Sodium Transport in Durum Wheat. *Plant Physiol.* **2005**, *137*, 807–818. [[CrossRef](#)] [[PubMed](#)]
34. Cassaniti, C.; Leonardi, C.; Flowers, T.J. The effects of sodium chloride on ornamental shrubs. *Sci. Hortic.* **2009**, *122*, 586–593. [[CrossRef](#)]
35. Cuin, T.A.; Zhou, M.; Parsons, D.; Shabala, S. Genetic behaviour of physiological traits conferring cytosolic K^+/Na^+ homeostasis in wheat. *Plant Biol.* **2012**, *14*, 438–446. [[CrossRef](#)] [[PubMed](#)]
36. Carillo, P.; Mastrolonardo, G.; Nacca, F.; Parisi, D.; Verlotta, A.; Fuggi, A. Nitrogen metabolism in durum wheat under salinity: Accumulation of proline and glycine betaine. *Funct. Plant Biol.* **2008**, *35*, 412–426. [[CrossRef](#)]
37. Fraire-Velázquez, S.L.; Balderas-Hernández, V.E. Abiotic Stress in Plants and Metabolic Responses. In *Abiotic Stress—Plant Responses and Applications in Agriculture*; Vahdati, K., Leslie, C., Eds.; InTech: Rijeka, Croatia, 2013. [[CrossRef](#)]
38. Goodrich, B.; Koski, R.R.; Jacobi, W. Roadside vegetation health condition and magnesium chloride ($MgCl_2$) dust suppressant use in two Colorado, U.S. Counties. *Arboric. Urban. For.* **2008**, *34*, 252.
39. Geilfus, C.M. Chloride: From nutrient to toxicant. *Plant Cell Physiol.* **2018**, *59*, 877–886. [[CrossRef](#)] [[PubMed](#)]
40. Britto, D.T.; Kronzucker, H.J. Futile cycling at the plasma membrane: A hallmark of low-affinity nutrient transport. *Trends Plant Sci.* **2006**, *11*, 529–534. [[CrossRef](#)]
41. Marschner, H. *Mineral Nutrition in Higher Plants*, 2nd ed.; Academic Press: London, UK, 1995. [[CrossRef](#)]
42. Xu, G.; Magen, H.; Tarchitzky, J.; Kafkafi, U.; Donald, L.S. Advances in chloride nutrition of plants. In *Advances in Agronomy*; Sparks, D.L., Ed.; Academic Press: San Diego, CA, USA, 1999; pp. 96–150.
43. Broadley, M.; Brown, P.; Cakmak, I.; Rengel, Z.; Zhao, F. Chapter 7—Function of Nutrients: Micronutrients. In *Marschner's Mineral Nutrition of Higher Plants*, 3rd ed.; Marschner, P., Ed.; Academic Press: San Diego, CA, USA, 2012; pp. 191–248.
44. Franco-Navarro, J.D.; Brumós, J.; Rosales, M.A.; Cubero-Font, P.; Talón, M.; Colmenero-Flores, J.M. Chloride regulates leaf cell size and water relations in tobacco plants. *J. Exp. Bot.* **2016**, *67*, 873–891. [[CrossRef](#)]
45. Tavakkoli, E.; Rengasamy, P.; McDonald, G.K. High concentrations of Na^+ and Cl^- ions in soil solution have simultaneous detrimental effects on growth of faba bean under salinity stress. *J. Exp. Bot.* **2010**, *61*, 4449–4459. [[CrossRef](#)]
46. Tavakkoli, E.; Fatehi, F.; Coventry, S.; Rengasamy, P.; McDonald, G.K. Additive effects of Na^+ and Cl^- ions on barley growth under salinity stress. *J. Exp. Bot.* **2011**, *62*, 2189–2203. [[CrossRef](#)]
47. Borgognone, D.; Roupael, Y.; Cardarelli, M.; Lucini, L.; Colla, G. Changes in biomass, mineral composition, and quality of cardoon in response to $NO_3^-:Cl^-$ ratio and nitrate deprivation from the nutrient solution. *Front. Plant Sci.* **2016**, *7*. [[CrossRef](#)] [[PubMed](#)]
48. Kumar, P.; Lucini, L.; Roupael, Y.; Cardarelli, M.; Kalunke, R.M.; Colla, G. Insight into the role of grafting and arbuscular mycorrhiza on cadmium stress tolerance in tomato. *Front. Plant Sci.* **2015**, *6*, 477. [[CrossRef](#)] [[PubMed](#)]
49. Roupael, Y.; Colla, G.; Giordano, M.; El-Nakhel, C.; Kyriacou, M.C.; De Pascale, S. Foliar applications of a legume-derived protein hydrolysate elicit dose-dependent increases of growth, leaf mineral composition, yield and fruit quality in two greenhouse tomato cultivars. *Sci. Hortic.* **2017**, *226*, 353–360. [[CrossRef](#)]
50. Bremner, J.M. Total nitrogen. In *Methods of Soil Analysis-Part 2*; Black, C.A., Ed.; American Society of Agronomy, Soil Science Society of America: Madison, WI, USA, 1965. [[CrossRef](#)]

51. Kyriacou, M.C.; El-Nakhel, C.; Graziani, G.; Pannico, A.; Soteriou, G.; Giordano, M.; Giordano, M.; Ritieni, A.; De Pascale, S.; Roupshael, Y. Functional quality in novel food sources: Genotypic variation in the nutritive and phytochemical composition of thirteen microgreens species. *Food Chem.* **2019**, *277*, 107–118. [[CrossRef](#)] [[PubMed](#)]
52. Ciarmiello, L.F.; Piccirillo, P.; Carillo, P.; De Luca, A.; Woodrow, P. Determination of the genetic relatedness of fig (*Ficus carica* L.) accessions using RAPD fingerprint and their agro-morphological characterization. *South Afr. J. Bot.* **2015**, *97*, 40–47. [[CrossRef](#)]
53. Carillo, P.; Cacace, D.; De Pascale, S.; Rapacciuolo, M.; Fuggi, A. Organic vs. traditional potato powder. *Food Chem.* **2012**, *133*, 1264–1273. [[CrossRef](#)]
54. Ju, J.H.; Yeum, K.J.; Son, H.M.; and Yoon, Y.H. Morphological and physiological responses of purple chrysanthemum (*Aster sphathulifolius*) under long-term stress of calcium chloride as deicing salt. *Appl. Ecol. Environ. Res.* **2018**, *16*, 605–616. [[CrossRef](#)]
55. Borghesi, E.; Carmassi, G.; Ugucconi, M.C.; Vernieri, P.; Malorgio, F. Effects of calcium and salinity stress on quality of lettuce in soilless culture. *J. Plant Nutr.* **2013**, *36*, 677–690. [[CrossRef](#)]
56. Colla, G.; Roupshael, Y.; Jawad, R.; Kumar, P.; Rea, E.; Cardarelli, M. The effectiveness of grafting to improve NaCl and CaCl₂ tolerance in cucumber. *Sci. Hortic.* **2013**, *164*, 380–391. [[CrossRef](#)]
57. Borgognone, D.; Cardarelli, M.; Lucini, L.; Colla, G. Does CaCl₂ play a role in improving biomass yield and quality of cardoon grown in a floating system under saline conditions? *HortScience* **2014**, *49*, 1523–1528. [[CrossRef](#)]
58. Diatloff, E.; Roberts, M.; Sanders, D.; Roberts, S.K. Characterization of anion channels in the plasma membrane of Arabidopsis epidermal root cells and the identification of a citrate-permeable channel induced by phosphate starvation. *Plant Physiol.* **2004**, *136*, 4136–4149. [[CrossRef](#)] [[PubMed](#)]
59. Carillo, P.; Mastrolonardo, G.; Nacca, F.; Fuggi, A. Nitrate reductase in durum wheat seedlings as affected by nitrate nutrition and salinity. *Funct. Plant Biol.* **2005**, *32*, 209–219. [[CrossRef](#)]
60. Munns, R. Comparative physiology of salt and water stress. *Plant Cell Environ.* **2002**, *25*, 239–250. [[CrossRef](#)] [[PubMed](#)]
61. Touraine, B.; Clarkson, D.T.; Muller, B. Regulation of nitrate uptake at the whole plant level. In *A Whole Plant Perspective on Carbon-Nitrogen Interactions*; Roy, J., Garnier, E., Eds.; SPB Academic Publishing: Hague, The Netherlands, 1994; pp. 11–30.
62. Galangau, F.; Daniel-Vedele, F.; Moureaux, T.; Dorbe, M.F.; Leydecker, M.T.; Caboche, M. Expression of Leaf Nitrate Reductase Genes from Tomato and Tobacco in Relation to Light-Dark Regimes and Nitrate Supply. *Plant Physiol.* **1998**, *88*, 383–388. [[CrossRef](#)] [[PubMed](#)]
63. Foyer, C.H.; Valadier, M.H.; Migge, A.; Becker, T.W. Drought-induced effects on nitrate reductase activity and mRNA and on the coordination of nitrogen and carbon metabolism in maize leaves. *Plant Physiol.* **1998**, *117*, 283–292. [[CrossRef](#)] [[PubMed](#)]
64. Zhao, L.; Liu, F.; Crawford, N.M.; Wang, Y. Molecular regulation of nitrate responses in plants. *Intern. J. Mol. Sci.* **2018**, *19*, 2039. [[CrossRef](#)] [[PubMed](#)]
65. Soltabayeva, A.; Srivastava, S.; Kurmanbayeva, A.; Bekturova, A.; Fluhr, R.; Sagi, M. Early senescence in older leaves of low nitrate-grown atxdh1 uncovers a role for purine catabolism in N supply. *Plant Physiol.* **2018**, *178*, 1027–1044. [[CrossRef](#)]
66. Suhayda, C.G.; Redmann, R.E.; Harvey, B.L.; Cipywnyk, A.L. Comparative response of cultivated and wild barley species to salinity stress and calcium supply. *Crop. Sci.* **1992**, *32*, 154–163. [[CrossRef](#)]
67. Abel, G.H. Inheritance of the capacity for chloride inclusion and chloride exclusion by soybeans. *Crop. Sci.* **1969**, *9*, 697–698. [[CrossRef](#)]
68. Li, B.; Tester, M.; Gilliam, M. Chloride on the Move. *Trends Plant Sci.* **2017**, *22*, 236–248. [[CrossRef](#)]
69. Henderson, S.W.; Gilliam, M. The Gatekeeper Concept: Cell-Type Specific Molecular Mechanisms of Plant Adaptation to Abiotic Stress. In *Molecular Mechanisms in Plant Adaptation*; Laitinen, R.A., Ed.; Wiley-Blackwell: Hoboken, NJ, USA, 2015; pp. 83–115. [[CrossRef](#)]
70. Li, B.; Qiu, J.; Jayakannan, M.; Xu, B.; Li, Y.; Mayo, G.M.; Tester, M.; Gilliam, M.; Roy, S.J. AtNPF2.5 modulates chloride (Cl⁻) efflux from roots of *Arabidopsis thaliana*. *Front. Plant Sci.* **2017**, *7*, 2013. [[CrossRef](#)] [[PubMed](#)]

71. Wege, S.; Jossier, M.; Filleur, S.; Thomine, S.; Barbier-Brygoo, H.; Gambale, F.; De Angeli, A. The proline 160 in the selectivity filter of the Arabidopsis NO_3^-/H^+ exchanger AtCLCa is essential for nitrate accumulation in planta. *Plant J.* **2010**, *63*, 861–869. [[CrossRef](#)] [[PubMed](#)]
72. Wegner, L.H.; Raschke, K. Ion channels in the xylem parenchyma of barley roots—A procedure to isolate protoplasts from this tissue and a patch-clamp exploration of salt passageways into the xylem vessels. *Plant Physiol.* **1994**, *105*, 799–813. [[CrossRef](#)] [[PubMed](#)]
73. Teakle, N.L.; Tyerman, S.D. Mechanisms of Cl^- transport contributing to salt tolerance. *Plant Cell Environ.* **2010**, *33*, 566–589. [[CrossRef](#)] [[PubMed](#)]



© 2019 by the authors. Licensee MDPI, Basel, Switzerland. This article is an open access article distributed under the terms and conditions of the Creative Commons Attribution (CC BY) license (<http://creativecommons.org/licenses/by/4.0/>).